J Mater Sci (2006) 41:8144–8151
DOI 10.1007/s10853-006-0170-0

Bioactive ceramic coatings containing carbon nanotubes on metallic substrates by electrophoretic deposition

I. Singh · C. Kaya · M. S. P. Shaffer · B. C. Thomas · A. R. Boccaccini

Received: 7 February 2006 / Accepted: 4 April 2006 / Published online: 28 October 2006

Abstract A range of potentially bioactive ceramic coatings, based on combinations of either hydroxyapatite (HA) or titanium oxide nanoparticles with carbon nanotubes (CNTs), have been deposited on metallic substrates, using electrophoretic deposition (EPD). Sol–gel derived, ultrafine HA powders (10–70 nm) were dispersed in multi-wall nanotube-containing ethanol suspensions maintained at pH = ~3.5 and successfully coated onto Ti alloy wires at 20 V for 1–3 min For TiO_2/CNT coatings, commercially available titania nanopowders and surface-treated CNTs in aqueous suspensions were co-deposited on stainless steel planar substrates. A field strength of 20 V/cm and deposition time of 4 min were used working at pH = 5. Although the co-deposition mechanism was not investigated in detail, the evidence suggests that co-deposition occurs due to the opposite signs of the surface charges (zeta potentials) of the particles, at the working pH. Electrostatic attraction between CNTs and TiO_2 particles leads to the creation of composite particles in suspension, consisting of TiO_2 particles homogenously attached onto the surface of individual CNTs. Under the applied electric field, these net negatively charged ''composite TiO_2/CNT'' elements migrate to and deposit on the anode (working electrode). The process of EPD at constant voltage conditions was optimised in both systems to achieve homogeneous and reasonably adhered deposits of varying thicknesses on the metallic substrates.

I. Singh · C. Kaya
Wolfson Centre for Materials Processing and Department of Mechanical Engineering, School of Engineering, Brunel University, West London, Uxbridge UB8 3PH, UK

M. S. P. Shaffer
Department of Chemistry, Imperial College London, South Kensington Campus, London SW7 2AZ, UK

B. C. Thomas · A. R. Boccaccini (✉)
Department of Materials, Imperial College London, Prince Consort Road, London SW7 2BP, UK
e-mail: a.boccaccini@imperial.ac.uk

Introduction

Hydroxyapatite (HA) is both bioactive and osteoconductive, making it a very attractive material for biomedical applications in orthopaedics. HA is usually processed via a powder route where sintering at a relatively high temperature is required for strengthening and densification of the component. High temperature treatment may result in the decomposition of the desirable HA structure reducing the bioactivity of the material [1]. Fine-grained nanopowders are required to enhance the sinterability of HA at lower temperatures, but a processing technique is then needed that allows the assembly of the nanopowders for fabrication of dense bulk components and coatings. Similarly, coatings based on titanium oxide are being investigated for enhanced biocompatibility of metallic implants [2, 3]. The formation of titania coatings from nanoparticles has been shown to lead to improved bioactive behaviour and enhanced tissue attachment in comparison to coatings made from μm-sized particles [4].

EPD is known to be one of the most effective and efficient techniques to assemble fine particles [5–7]. This technique has received significant attention due to its simplicity in setup, low equipment cost, and capability to form complex shapes and patterns [8–9]. Electrophoretic deposition is also a potentially attractive process for obtaining bioceramic coatings from aqueous and non-aqueous solutions of nanoparticles on metallic surfaces. The application of EPD in the biomaterials area, in particular for obtaining HA and bioactive glass coatings on metallic implants, has been demonstrated [10–13].

Recently, EPD has begun to be explored for the deposition of carbon nanotubes (CNTs), on a variety of substrates [14–17]. Our group has shown that stable aqueous suspensions of surface functionalised multi-wall CNTs are suitable for EPD, at relatively low voltages (<50 V) and low deposition times (<10 min), producing highly ordered, uniform CNT deposits on metallic substrates [15, 16]. The application of CNTs in the general biomedical field has been discussed in the literature, including areas such as diagnostic tools and devices, biopharmaceutics, implantable devices, as well as in surgical aids and instruments [18]; however, there has been only limited work on the incorporation of CNTs into bioactive ceramic matrices and coatings for applications in orthopaedics or tissue engineering [19, 20].

In this work, we have investigated the electrophoretic deposition of nanostructured HA/CNTs and TiO_2/CNTs composites with the aim of developing improved bioactive coatings on metallic substrates for orthopaedic applications. Multi-wall CNTs obtained by the chemical vapour deposition method were used. HA nanopowders were synthesised by a sol–gel method while for titania coatings a commercially available TiO_2 nanopowder was used.

Experimental procedures

Preparation of HA nanopowder

The hydroxyapatite powder was prepared using a sol–gel technique. Commercially available $Ca(NO_3)_2.4H_2O$ and P_2O_5 were obtained from Fisher Scientific and used with a molar ratio of 10:3, to obtain the desired Ca/P ratio in hydroxyapatite. About 10 mL ethyl alcohol was used as solvent. The sequence of the dissolution of the precursors was not important although excessively rapid combination of precursor solutions resulted in precipitation. The combined precursor solution was stirred for 30 min, and slowly transformed into a gel over a further 30 min to a maximum of 2 h. The gel was then dried in an oven at 120 °C in air for 15 h. The reaction of $Ca(NO_3)_2.4H_2O$ with P_2O_5 in alcohol resulted in the formation of the gel. The resultant gel was found to be transparent.

Preparation of HA/CNTs suspensions and EPD experiments

For these experiments CNT (multi-wall) were purchased from NTP, Nanotech Port Co., Shenzhen, China. Suspensions of HA nanoparticles and CNTs at a total concentration of 1 g solid/100 mL were prepared in ethanol (99.86%) and treated in an ultrasonic bath for 60 min to ensure a good dispersion of the particles and CNTs. The pH of the suspensions was 3.5. The concentration of CNTs was adjusted to be 1 wt% of the total HA powder. EPD was carried out at room temperature under constant DC voltage (20 V) at deposition times between 1 min and 3 min. A Ti alloy wire (1 mm in diameter) was used as the anode (deposition electrode) and a cylindrical stainless steel electrode was used as cathode (counter electrode).

Preparation of TiO_2/CNTs suspensions and EPD experiments

For this part of the investigation, multi-walled CNTs were grown in house using chemical vapour deposition (CVD) [21, 22]. Acid oxidation was used to produce aqueous CNT suspensions as reported previously [15]. Briefly, 0.8 g of nanotubes were refluxed in 60 mL of mixed (1:3) concentrated nitric and sulphuric acids at 130 °C for 30 min, following by washing to pH 7. After treatment, 50% of the nanotubes remained. The suspension was then centrifuged, to remove any remaining agglomerates, at 3,000 rpm for 30 min, producing an approximately 1 mg/mL aqueous suspension of CNTs. The suspension was further diluted to 0.58 mg/mL for use in EPD experiments. Stainless steel rectangular plates (RS Components, Nothants, UK) with dimensions of $1.2 \times 1.2 \times 0.2$ cm^3 were used both as the substrate (working electrode) and the counter electrode, in a purpose built EPD cell with an electrode separation of 2 cm. The electrodes were degreased with acetone prior to deposition. Optimisation of the EPD voltage was carried out in the range 5–50 V using suspensions containing only CNTs. For each deposition series, the voltage was kept constant while the deposition time was varied from 60 s to 600 s.

For preparation of titania/CNT coatings, commercially available TiO_2 nanopowder (P25, Degussa,

Germany) of mean particle size 23 nm was used. A suspension was made by mixing 3.5 g of TiO_2 nanopowder with 31.5 g of CNT aqueous solution (of 0.6 mg/mL CNTs concentration); the final stock suspension consisted of 10 wt% of TiO_2 nanoparticles and 90 wt% CNTs aqueous suspension. An ultrasonic bath was used to improve dispersion and to separate possible agglomerates. pH values were measured using a JENWAY 3510 pH metre, and adjusted by adding either sodium hydroxide (NaOH), or hydrochloric acid (HCl). The pH was adjusted to pH 5 after a trial-and-error approach. The EPD conditions were chosen following the results of the pure CNT deposition experiments, as described above.

After deposition, the coated electrodes were removed from the cell and dried at room temperature in air under ambient humidity. The electrodes were dried in horizontal position to improve homogeneity of the deposit. Samples were stored in a dessicator to prevent any degradation of the coatings.

Characterization

The microstructure of the synthesised HA powder was observed by scanning electron microscopy (SEM, JEOL JSM-840) equipped with EDX analysis. The powder samples were mounted on Al stubs and gold-coated before being subjected to SEM analysis. Pure CNT, HA/CNTs and TiO_2/CNT coatings were gold-coated (Emitech K450 apparatus) and examined using a Field Emission Gun SEM (FEG-SEM, Leo Gemini) to determine microstructure and thickness. Samples for SEM analysis were either imaged directly or embedded in epoxy and polished. Samples embedded in epoxy were ground to expose a complete cross-section, using silicon carbide paper, and then polished using 3 μm and 1 μm diamond pastes. Transmission Electron Microscopy (JEOL 2000 FX) samples were prepared from powders ultrasonically agitated for few minutes in ethanol and collected on a carbon film.

Fourier transformed infrared (FTIR) spectroscopy (Perkin-Elmer Instruments) was performed on HA coatings to establish HA stoichiometry, i.e., to confirm the absence or presence of partially substituting PO_4^{3-} and/or OH^- groups. In order to study the phase evolution and formation of crystalline HA, the as-dried powder was analysed by TGA/DSC in N_2 atmosphere using a TA instrument. Phase analysis of the synthesised HA powders was conducted using an X-ray diffractometer (Phillips) using Cu Kα radiation (λ = 1.5418A).

Results and discussion

Starting materials and suspensions

HA/CNTs system

Figure 1a shows an SEM image of the dried HA powder. The powder appears to be highly agglomerated due to the effects of surface tension during drying of the gel precursor and the very fine nature of the HA powders. TEM demonstrates (Fig. 1b) the fine particle size (10–50 nm) and the spherical shape of the primary particles.

Figure 2a and b show SEM micrographs of HA/CNTs mixtures at different magnifications. Figure 2a shows evidence of good intermixing of the HA powder and carbon nanotubes; no preferential agglomerates of HA powders or CNTs were observed in either SEM or TEM examination, confirming that the suspensions

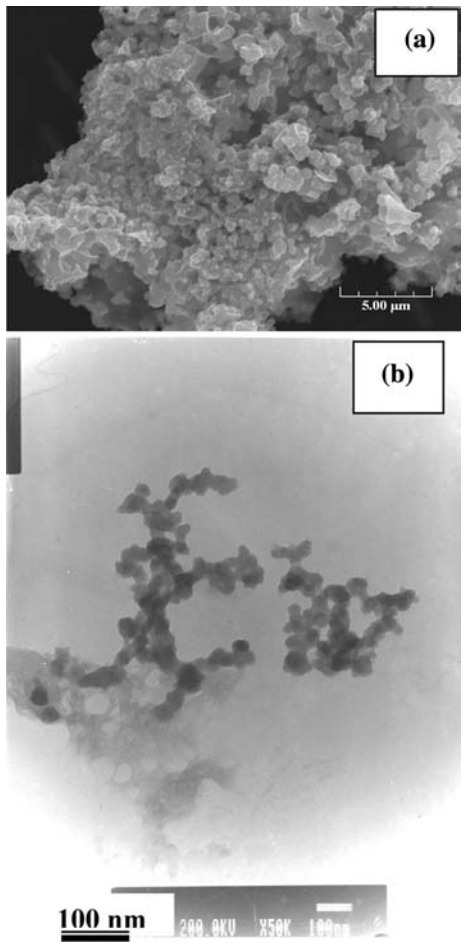

Fig. 1 (**a**) SEM and (**b**) TEM micrographs of synthesised HA powders

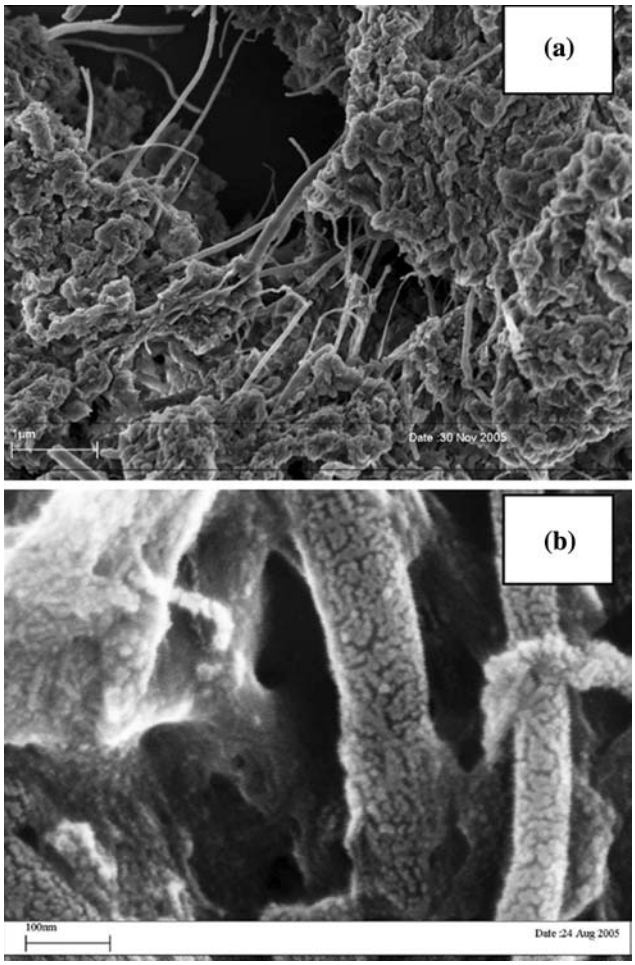

Fig. 2 SEM micrographs of HA/CNTs powder mixtures at (**a**) low and (**b**) high magnifications

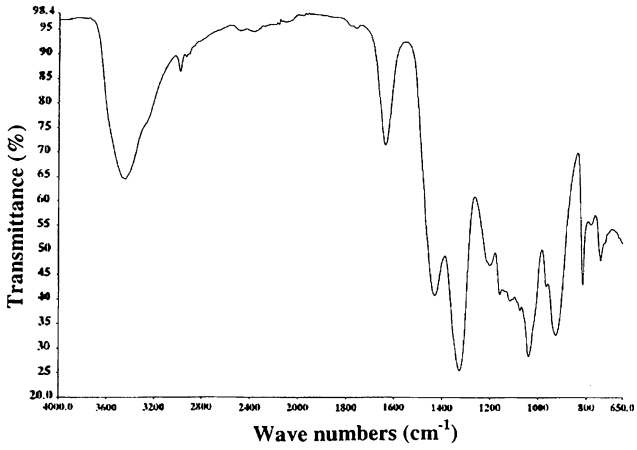

Fig. 3 FTIR spectrum of as-synthesised HA powders

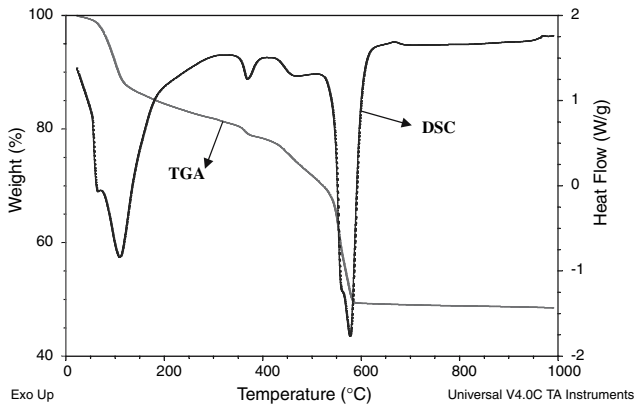

Fig. 4 Thermo-gravimetric analysis and differential scanning calorimetry of the HA powder

used were well dispersed and stable. In addition, ultrafine HA particles, smaller than ~10 nm, were observed uniformly coating the surface of the CNTs, as shown in Fig. 2b. A study is currently being conducted to determine the details of interaction of HA particles and CNTs as a function of pH.

The FTIR spectrum of the HA powder exhibited the characteristic peaks corresponding to OH^- (650 cm^{-1} and 4,000 cm^{-1}) and PO_4^{3-} (960, 1,050, 1090 cm^{-1}), together with the weak bands of the CO_3^{2-} group (870, 1,415, 1,450 cm^{-1}), as shown in Fig. 3.

Figure 4 shows the result of a thermogravimetric analysis combined with differential scanning calorimetry (TGA/DSC) conducted on the as-dried HA gel powder. The reaction between $Ca(NO_3)_2.4H_2O$ and P_2O_5 is known to form amorphous HA; the P_2O_5 reacts with alcohol to from $P(O)(OR)_3$ oxyalkoxide with the liberation of water, which in turn partially hydrolyzes the oxyalkoxide precursors. The presence of phosphorous hydroxyl-alkoxide itself is not sufficient to form a gel, which indicates the important role of $Ca(NO_3)_2.4H_2O$.

The first indication of weight loss, where a broad endothermic peak is observed in the TGA curve (~200 °C), appears to correspond to the evaporation of crystalline bonded water present in $Ca(NO_3)_2.4H_2O$. This weight loss is also associated with the removal of nitrate and ammonium from the powders. Small weight losses between 100 °C and 200 °C probably relate to the evaporation of ethanol. The second sharp weight loss combined with a sharp endothermic peak (~425 °C) implies the removal of residual NO_3 groups although there are other small endothermic peaks in the ~250–300 °C range, the origin of which is not clear at present. These endothermic peaks could be related to one or more of the alkoxy-nitrate species in the precursor, but are more likely caused by the removal of (combinations of) other groups in the precursor, such as –OH. The sharp exothermic peak at ~325 °C corresponds to the crystallization of HA.

There is no significant weight loss observed above 550 °C, indicating that the precursor generates a stable phase after this heat treatment. The phase evolution behaviour of the synthesised HA powder after sintering at 600 °C for 2 h is reflected in the XRD data in Fig. 5, which confirms the presence of stoichiometric HA matching JCPDS standards. Only crystalline HA phase was detected in the sintered sample.

TiO_2/CNTs

A plausible hypothesis for the co-depostion of TiO_2 and CNTs from mixed suspensions is as follows. The isoelectric point of TiO_2 suspensions in water is at pH 5 [23], whilst that of oxidised CNTs is known to be at pH < 2 [24]. By working at a pH where CNTs and TiO_2 nanoparticles exhibit surface charges of opposite sign (~2 < pH < 5), positively charged TiO_2 nanoparticles should be attracted to the negatively charged CNTs [15], ideally forming individual, TiO_2-coated CNTs; these composite elements can then migrate to the anode. The detailed description of the suspension stability and the zeta potential versus pH curves is the focus of a parallel investigation; however, TEM observations of CNT/TiO_2 combinations confirm that the hypothesis is realistic (see Fig. 6).

Electrophoretic deposition

HA/CNTs composites

Figure 7a–c show SEM micrographs of HA/CNTs films electrophoretically deposited on Ti alloys using a constant voltage of 20 V and varying deposition times. After one minute of deposition, the thickness of the

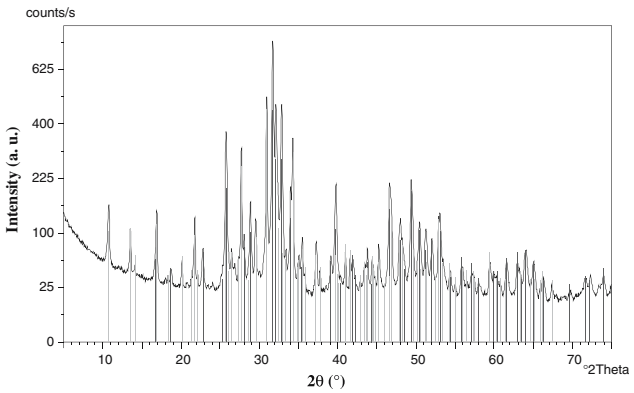

Fig. 5 X-ray diffraction results of HA powders sintered at 600 °C for 2 h showing the high crystallinity of the powder. Peaks are seen to match crystalline stoichiometric HA (JCPDS standards)

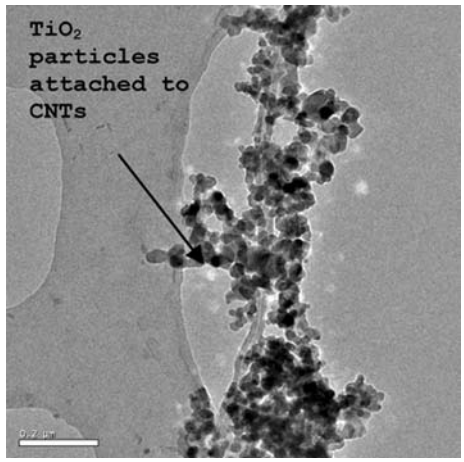

Fig. 6 TEM micrograph showing the interaction between TiO_2 nanoparticles and CNTs in aqueous suspensions at pH < 5

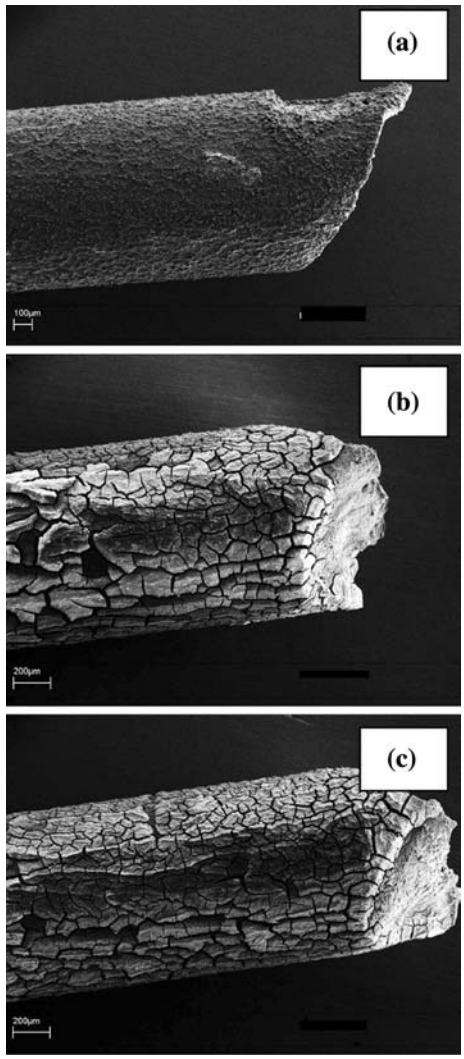

Fig. 7 SEM micrographs of HA/CNTs coated Ti alloy wire as a function of deposition time, (**a**) 1 min, (**b**) 2 min, (**c**) 3 min

coating layer was about 12 μm and no cracks were observed on the surface. However, film thickness increased with deposition time, resulting in multiple cracking on drying. Different drying techniques are being currently investigated to eliminate this problem.

At higher magnification (Fig. 8a), SEM suggests a good dispersion and intimate mixing between HA particles and CNTs. EDX analysis (Fig. 8b) supports the suggestion that both HA and CNTs are present in the deposit. The exact concentration of CNTs has not been determined quantitatively but microscopy observations indicate this to be of the order of 1 wt%.

TiO_2/CNTs composites

The optimisation of the electrophoretic deposition parameters for the aqueous CNT suspensions used in this part of the investigation was described in detail in a previous study [16]. The deposition of acid-treated CNTs occurs at the anode [15, 16]. The acid-treatment of the CNTs provides this negative surface charge by introducing carboxylic and other oxygen-containg groups [25]. Direct visual examination of the CNT films after drying indicated that the coating quality was dependent on the deposition time, the deposition voltage, and the drying conditions. In general, for the present system and EPD conditions, the higher the voltage, the better the quality of the deposit, as previously observed [15]. However very high voltages might lead to non-uniform coatings and uncontrolled microstructures [26]. For best quality of the deposits, the contacts to the electodes should not be immersed in the EPD suspension. It was found that a field strength of 20 V/cm and deposition times 4 min led to relatively thick CNT deposits of sufficient microstructural homogeneity, as also discussed elsewhere [16]. Figure 9a, b show SEM images of a typical CNT deposit obtained by applying optimal EPD parameters, in top view and cross section, respectively. The homogeneous microstructure of the deposit as well the uniform deposit thickness of ~15 μm can be observed.

The same parameters were used to co-deposit CNTs and TiO_2 nanoparticles. SEM (Fig. 10a) shows that the TiO_2/CNT coatings have a homogenous structure.

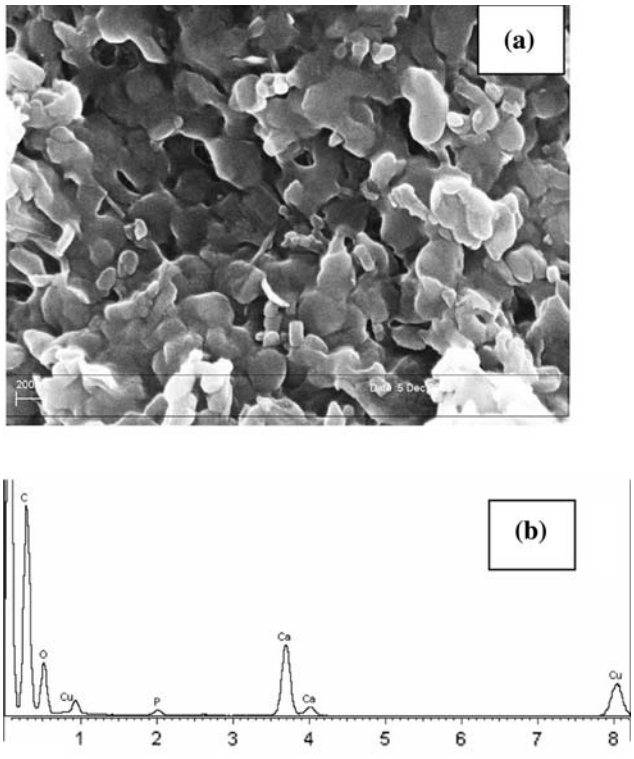

Fig. 8 (**a**) SEM micrograph of HA/CNTs deposit on Ti alloy wire at high magnification, and (**b**) corresponding EDX spectra

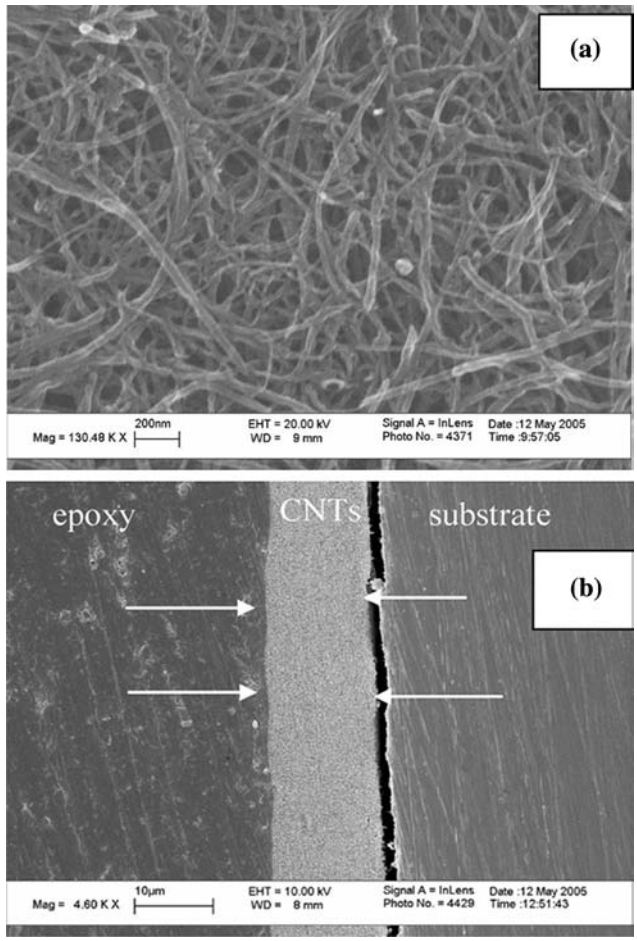

Fig. 9 FEG-SEM images of stainless steel substrates coated with CNTs by EPD at 20 V/cm for 4 min: (**a**) direct image of CNT coating surface at high magnification (**b**) polished surface mounted in epoxy resin showing CNT coating thickness (marked by arrows)

Samples (including that shown) were intentionally fractured in order to reveal the CNTs pulled-out of the fracture surface. At higher magnification (Fig. 10b), it is possible to observe TiO_2 nanoparticles deposited on the surface of individual CNTs, which are emerging in perpendicular direction to the surface of the deposit. This particular nanostructured surface is expected to be suitable for the attachment and subsequent proliferation of cells, thus the deposits are potentially high bioactive materials. The microstructural and mechanical characterisation of these composite deposits is the subject of current investigations. It should be finally pointed out that the combination of CNTs and nanocrystalline particles has applications in a broad range of fields beyond biomaterials such as in field emission displays, nanoelectronic devices, antibacterial films, biosensors, photocatalytic nanostructures and in other functional composites [7, 27].

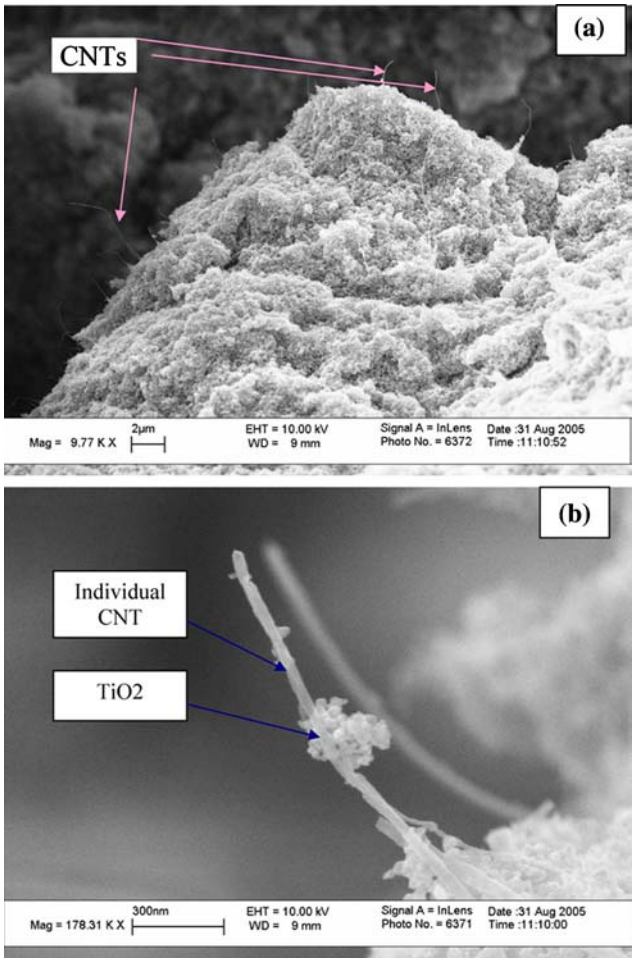

Fig. 10 FEG-SEM image of (**a**) a TiO_2/CNT composite coating obtained by EPD on a planar stainless steel substrate. The coating was intentionally fractured in order to reveal a view of the coating fracture surface, CNTs are observed pointing out of the fracture surface (marked by arrows), (**b**) high magnification view showing TiO_2 nanoparticles attached to CNTs oriented perpendicularly to the deposit surface

Conclusions

The EPD technique was used to produce potentially bioactive, nanostructured, ceramic, HA/CNT and TiO_2/CNT composite coatings on metallic substrates. To the authors' knowledge, this paper is the first report of EPD co-deposition of CNTs and ceramic nanoparticles to form a composite ceramic coating on metallic substrates of different shapes (wires or planar surfaces). Deposition voltage and time determine the thickness and homogeneity of coatings. Increasing deposition time leads to increased coating thickness which, in turn, causes microcracking upon drying. For the particular suspension used in the HA/CNTs system, 1 min was found to be enough to produce a deposit layer of 10 μm using a constant dc voltage of 20 V. SEM analysis of the coated Ti alloy wire showed adherent and uniform HA/CNTs coatings. Commercially available titania nanopowders and oxidised CNTs in aqueous suspensions were electrophoretically co-deposited on stainless steel planar substrates. Although the mechanisms of co-deposition of CNTs and TiO_2 nanoparticles were not investigated in detail, it is reasonable to assume that co-deposition occurs due the opposite surface charge of CNTs and TiO_2 particles in aqueous suspensions at $\sim 2 < pH < 5$ leading to attachment of TiO_2 particles on individual CNTs. The following parameters, electric field 20 V/cm, deposition time 4 min, led to homogeneous and uniform TiO_2/CNT coatings. The sintering and densification behaviour of TiO_2/CNT coatings needs to be investigated, although full densification is not necessary for applications where a porous surface is advantageous for improved attachment to living tissue. Further characterisation of the coatings is required for assessing their possible applications in the biomedical field; studies should include both mechanical and biological properties.

Acknowledgements EPSRC is acknowledged for financial support. Experimental assistance of Mr Feras Yosef is appreciated.

References

1. Wei M (1999) J Biomed Mater Res 45:11
2. Heidenau F, Mittelmeier W, Detsch R, Haenle M, Stenzel F, Ziegler G, Gollwitzer H (2005) J Mater Sci Mater Med 16:883

3. Ramires PA, Romito A, Cosentino F, Milella E (2001) Biomaterials 22:1467
4. Gutwein LG, Webster TK (2002) J Nanoparticulate Res 4:231
5. Kaya C, Kaya F, Su B, Thomas BJC, Boccaccini AR (2005) Surf Coat Tech 2–3:303
6. Tabellion J, Clasen R (2004) J Mater Sci 39:803
7. Boccaccini AR, Roether JA, Thomas BJC, Shaffer MSP, Chavez E, Stoll E, Minay EJ (2006) J Ceram Soc Japan 114:1
8. Van Der Biest O, Vandeperre L (1999) Ann Rev Mater Sci 29:327
9. Boccaccini AR, Zhitomirsky I (2002) Curr Opin Solid State Mater Sci 6:251
10. Zhitomirsky I, Gal-Or L (1997) J Mater Sci: Mater Med 8:213
11. Wei M, Ruys AJ, Milthorpe BK, Sorrell CC (2005) J Mater Sci Mater Med 16:319
12. Chen F, Lin LW, Lin CJ, Lu WW (2005) Key Eng Mater 288–289:183
13. Krause D, Thomas BC, Leinenbach C, Eifler D, Minay EJ, Boccaccini AR (2006) Surf Coat Tech 200:4835
14. Du CS, Heldebrant D, Pan N (2002) J Mater Sci Lett 21:565
15. Thomas BJC, Boccaccini AR, Shaffer MSP (2005) J Amer Cer Soc 88:980
16. Thomas BJC, Shaffer MSP, Freeman S, Koopman M, Chawla KK, Boccaccini AR (2006) Key Eng Mater 314:141
17. Gao B, Yue GZ, Qiu Q, Cheng Y, Shimoda H, Fleming L, Zhou O (2001) Adv Mater 13:1770
18. Sinha N, Yeow JTW (2005) IEEE Trans Nanobiosci 4:180
19. Correa-Duarte MA, Wagner N, Rojas-Chapana J, Morsczeck C, Thie M, Giersig M (2004) Nano Lett 4:2233
20. Zao L, Gao L (2004) Carbon 42:423
21. Rao CNR, Govindaraj A (1998) Mater Res Innov 2:128
22. Singh C, Shaffer MSP, Windle AH (2003) Carbon 41:359
23. Wang N, Lin H, Li J, Yang X, Chi B (2006) Thin Solid Films 496:649
24. Esumi K, Ishigami M, Nakajima A, Sawada K, Honda H (1996) Carbon 34:279
25. Shaffer MSP, Fan X, Windle AH (1998) Carbon 36:1603
26. Ma J, Chen J (2002) J Am Ceram Soc 85:1735
27. Lee S, Sigmund S (2003) Chem Commun 4:780